

## Simulating the Arm Movements of a Stepper Motor Controlled Pick-and-Place Robot Using the Stepper Motor Model

R. V. Sharan<sup>1</sup> and G. C. Onwubolu<sup>2</sup>

<sup>1</sup>*School of Engineering and Physics, University of the South Pacific, Suva, Fiji*

<sup>2</sup>*Knowledge Management and Mining, Toronto, Canada*

<sup>1</sup>*sharan\_r@usp.ac.fj, <sup>2</sup>onwubolu\_g@dsgm.ca*

### Abstract

*This paper describes the simulation of arm movements of a stepper motor controlled pick-and-place robot using the mathematical model of a stepper motor. The model includes: a) a model of the stepper motor driver board, b) a model of the hybrid stepper motor and load combination, and c) the interconnection of the two models which is used to simulate the motions of the base, shoulder, elbow, and wrist (pitch) motions of the pick-and-place robot. The model is simulated using Simulink and the results of angular displacement from the simulation and actual measurements show good uniformity.*

**Keywords:** *pick-and-place robot, modeling, simulation, hybrid stepper motor (HSM)*

### 1. Introduction

Pick-and-place operations, such as palletizing [1], are one of the many applications of robotic manipulators. They are often employed to increase productivity in a setting where tasks can be repetitive and laborious such as packaging [2] and assembly operations [2-4]. Application can also be in removing humans from hazardous work, such as the use of robotic arms in nuclear decommissioning tasks [5], and the increased level of intelligence integrated in some robotic arms of today means they can even work in collaboration with humans [6, 7].

While the operations of a pick-and-place robot can be customized by appropriate programming, developing an accurate model to simulate the motions of the robot can be used to determine the reach and efficiency of the robot, estimate cycle time, and convey potential collision paths without any actual implementation on hardware. This can save time and money and also prevent possible damage to the robot.

Servo motors are mostly used in the design of low payload pick-and-place robots and so most existing models are based on servo systems. This work, however, presents the modeling and simulation of a hybrid stepper motor (HSM) controlled pick-and-place robot. Stepper motors find usage in some high precision applications such as in computer numerically controlled (CNC) drilling, milling, and lathe machines. Motivation from this was used to develop a pick-and-place robot, which is presented in [8, 9], whereby stepper motors are used as actuators for the base, shoulder, elbow, and wrist (pitch) motions of the robot.

A stepper motor model for dynamic simulation has been presented by Morar [10] which uses a pulse generator to model the stepper motor driver board connected to the model of a two-phase stepper motor. A similar model was adapted by Chand *et al.*, [11] to model the axis movement of a CNC drilling machine but with four-phase HSMs used as the actuation device for the *X* and *Y* axis. The model includes: (a) a model of the stepper motor driver board, (b) a model of the four-phase HSM and load combination, (c) a model of angular to linear

movement conversion and (d) the interconnection of all three models to form the complete model of the X or Y axis drive which are similar.

This work takes a similar approach and uses the model of the stepper motor driver board and the model of the four-phase HSM to simulate the arm movements of the pick-and-place robot.

## 2. System Description

The mechanical structure of the developed robot is quite similar to the commercially available robotic arm Scorbot ER-4u and is to be employed in a smart flexible manufacturing system (SFMS) which consists of a machining center in the form of a CNC drilling machine [12]; a transportation system in the form of an automatic guided vehicle (AGV) [13]; and the pick-and-place robot [8, 9]. The remote machining system is based on Internet technology such that the CNC drilling machine could be controlled by registered and authenticated clients from any part of the world [14].

The framework for the developed pick-and-place robot is shown in Figure 1. A vision system is integrated into the workspace of the pick-and-place robot to recognize the shape and color of work-pieces on the work-plane of the robot. The user specifies the shape and color of the work-pieces to be manipulated through a graphical user interface (GUI) and the robot, based at the machining center, unloads the specified work-pieces from the work-plane, on the AGV, to the machining center for drilling operations.

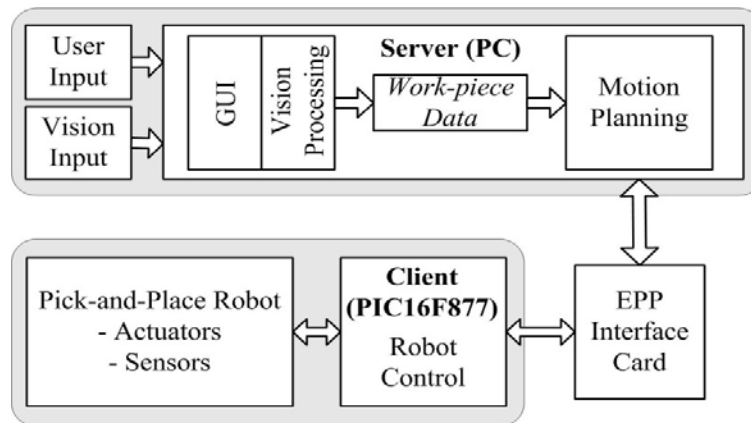


**Figure 1. Framework for the Pick-and-place Robot**

Furthermore, the robot is controlled by a PIC16F877 microcontroller which allows easy interface to the control electronics. However, for motion planning and since the overall project also involves image processing, sufficient additional processing power is provided in the form of a personal computer (PC), designated as a server. Output data from motion planning is then communicated on request through the enhanced parallel port (EPP) of the PC to the PIC microcontroller, acting as the client, which actuates the robot and interfaces with the sensing devices. The client-server control architecture has been presented in [15].

The pick-and-place robot has been developed for operation in an indoor environment and is mounted on a worktable which is fixed with respect to the work-plane. It has been designed for handling light weight and small size material such as wax, wood, and aluminum and therefore has a limited payload of 0.5 kg. It offers five degree-of-freedom (DOF) with motions about the base, shoulder, and elbow joints together with pitch and roll motions at the

wrist joint. Also, a two-finger gripper is used as the end-of-arm-tool (EOAT) for firmly gripping the work-piece while it is being moved from one position to another.

HSM is used as the actuation device for the base, shoulder, elbow, and wrist (pitch) motions of the pick-and-place robot. Each of these motions are similar and the main subsystems of the open-loop HSM drive are shown in Figure 2. The outputs from the PIC microcontroller are the input commands to the stepper motor drive board in the form of clock pulse and direction signal. The subsystems are discussed in the following subsections.

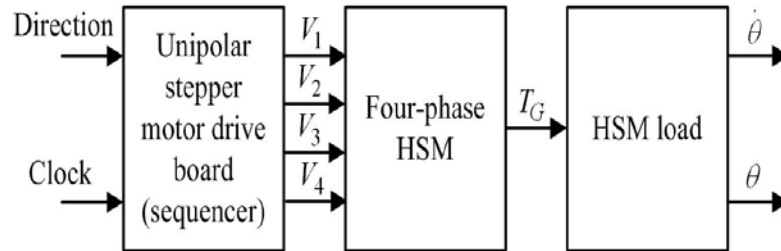


**Figure 2. Main Subsystems of the Stepper Motor Drive**

### 2.1. Unipolar Stepper Motor Drive Board

The unipolar stepper motor drive board (RS stock 217-3611) has been used in this work and more details on this can be found in [16]. The drive board has been modeled as a sequencer where the voltage applied to each phase of the HSM is represented using square wave pulses following the excitation sequence provided in [17]. The frequency of the square wave pulses is same as the clock frequency which also acts as a clock enable. Table 1 shows the excitation sequence for the four-phases of the HSM for clockwise rotation of the motor shaft.

**Table 1. Excitation Sequence for Clockwise Rotation**

	Step	Phase 1 $\phi_1 = 0$	Phase 2 $\phi_2 = \pi$	Phase 3 $\phi_3 = \pi/2$	Phase 4 $\phi_4 = 3\pi/2$
Start	1	On		On	
	2		On	On	
	3		On		On
	4	On			On
Repeat 1	5	On		On	

### 2.2. HSM and Load Combination

HSM (RS stock 440-442) [17] has been used in this work. Hybrid stepper motors provide high stepping rates ( $1.8^\circ$ ) and high working torque compared to permanent magnet ( $7.5^\circ$  and  $15^\circ$ ) types. Their ability to maintain a high detent torque even when not energized makes them an ideal choice for position integrity and so eliminating the need for position feedback. HSMs with a torque rating of 500 mNm were coupled with appropriate gear box, based on the torque requirement for each motion, and controlled using unipolar drive boards. A summary of the input frequency to the unipolar board is given in Table 2 along with the gear ratio of the HSM gearbox and the ratio of the gear and/or timing pulley linking the motor shaft to the joint for each motion.

**Table 2. Summary of Input Frequency and Gear Ratio**

Motion	Input frequency (Hz)	Gearbox ratio, $k_1$	Gear and/or timing pulley ratio, $k_2$
Base	50	5:1	22:44
Shoulder	500	25:1	18:78
Elbow	125	25:2	13:22
Wrist (pitch)	500	25:1	13:22

The model of the HSM used in this work is based on the model described by Chand *et al.*, [11].

The number of rotor teeth of the HSM is given by

$$\text{step length} = \frac{90^\circ}{p} \quad (1)$$

where  $p$  is the number of rotor teeth. The basic time domain equations for each phase of the HSM can be expressed as equations (2), (3) and (4):

$$v_j = R_j i_j + L_j \frac{di_j}{dt} + e_j \quad (2)$$

where  $v_j$ ,  $R_j$ ,  $i_j$ ,  $L_j$ , and  $e_j$ , are the voltage, resistance, current, inductance and induced electromotive force (e.m.f.) for phase  $j$  respectively;

$$e_j = k_m \sin(p\theta_1 + \phi_j) \dot{\theta}_1 \quad (3)$$

where  $k_m$ ,  $\theta_1$  and  $\dot{\theta}_1$  are the motor constant, angular displacement and angular velocity of the HSM respectively and, additionally,  $\phi_j$  is the location of phase  $j$  in the stator;

$$\tau_{Mj} = k_m \sin(p\theta_1 + \phi_j) i_j \quad (4)$$

where  $\tau_{Mj}$  is the contribution of phase  $j$  towards the motor's torque.

Equation (2) is a differential equation and can be expressed in the Laplace domain as

$$V_j - E_j = R_j I_j + sL_j I_j \quad (5)$$

The total torque developed by the HSM (expressed in the Laplace domain),  $T_G$ , is

$$T_G = \sum_{j=1}^4 T_{Mj} \quad (6)$$

The HSM torque,  $T_G$ , which is amplified via a gearbox, is used to overcome friction and to accelerate the motor, gear, belt and pulley combination.

The relevant equation is

$$T_G = T_F + B_R \dot{\theta}_1 + J_R s \dot{\theta}_1 \quad (7)$$

where  $J_R$  is the lumped inertia of the motor, gear, belt and pulley combination and  $\dot{\Theta}_1$  is the angular velocity of the gear at the motor end, which is the angular velocity of the HSM expressed in the Laplace domain. The friction torque is modeled as the lumped Coulomb friction  $T_F$  and the lumped viscous friction coefficient  $B_R$ .

### 3. Overall Block Diagram

The overall block diagram for a single joint is shown in Figure 3 where equations (2) to (7) comprise the HSM and load combination. The numerical values for all parameters are given in Table 3. While some parameters were obtained from the manufacturer’s datasheet, others, such as  $k_m$ ,  $J_R$ ,  $B_R$ , and  $T_F$ , were obtained from [11].

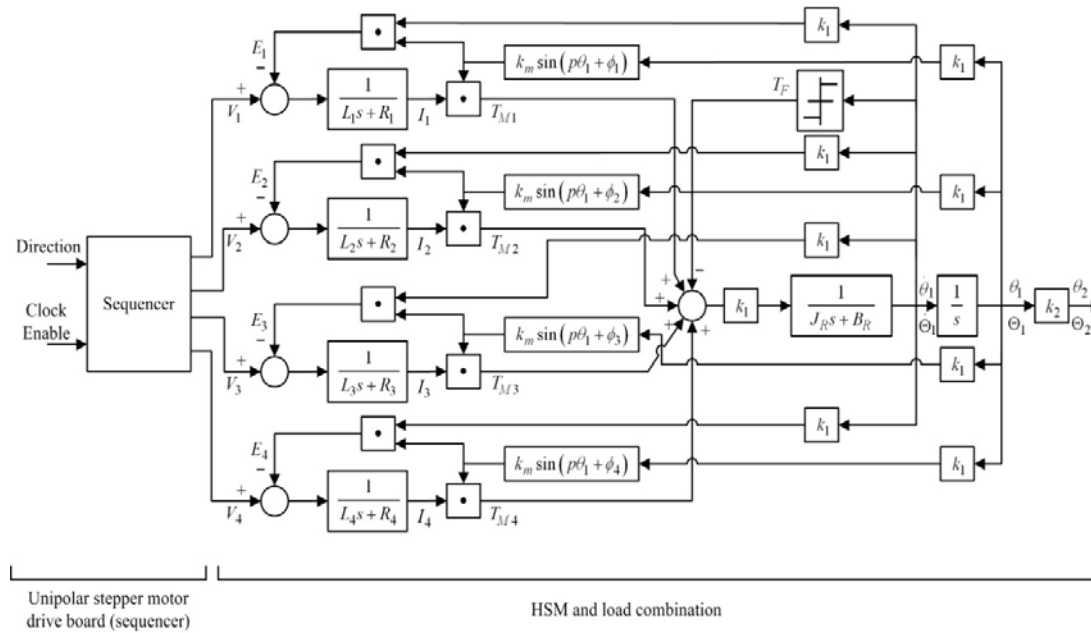


### Figure 3. Overall Block Diagram for a Single Joint

### Table 3. Block Diagram Parameter Numerical Values

Parameter	Value
$L_1, L_2, L_3, L_4$	0.009 H
$R_1, R_2, R_3, R_4$	5 $\Omega$
$k_m$	0.6 Nm/A
$p$	50
$\phi_1$	0
$\phi_2$	$\pi$
$\phi_3$	$\pi/2$
$\phi_4$	$3\pi/2$
$J_R$	0.00003 kgm <sup>2</sup>
$B_R$	0.02 Nms
$T_F$	0.1 Nm

## 4. Model Simulation and Validation

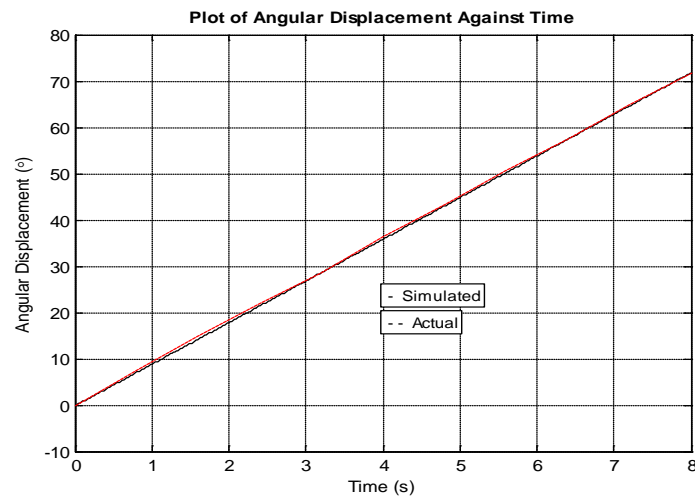
### 4.1. Model Simulation

The block diagram shown in Figure 3 was simulated using Simulink version 7.3, which is part of version 7.8.0.347 (R2009a) of MATLAB. The inputs of the simulation are clock enable and direction while the outputs are angular displacement and angular velocity of the respective arm of the robot.

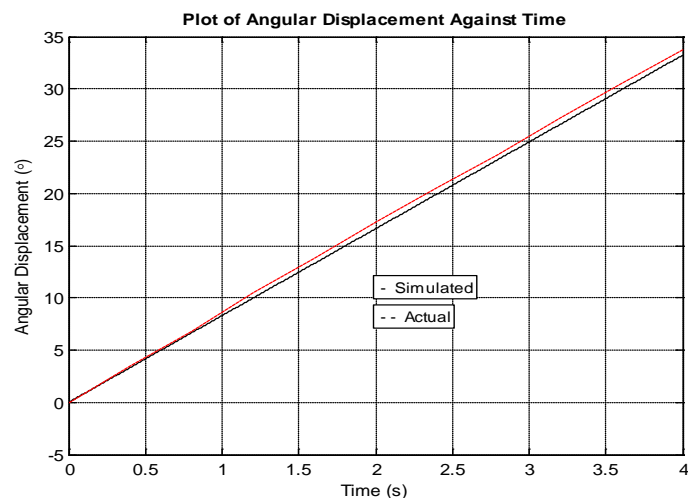
### 4.2. Model Validation

The angular velocity of the arm movements could not be physically measured due to limitations in instrumentation. Therefore, only the simulated and actual results for angular displacement were compared. In both cases, the direction was set to logic 0 for clockwise rotation of the motor shaft while the clock frequency was set as given in Table 2.

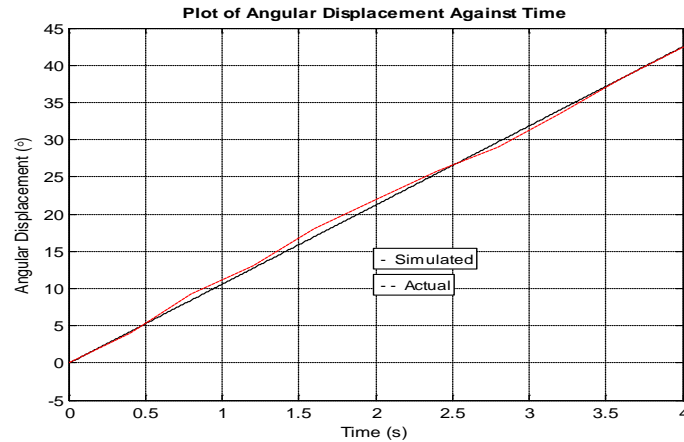
Figure 4 shows the simulated and actual robot arm angular displacements for (a) the base, (b) the shoulder, (c) the elbow, and (d) the wrist (pitch) motions.



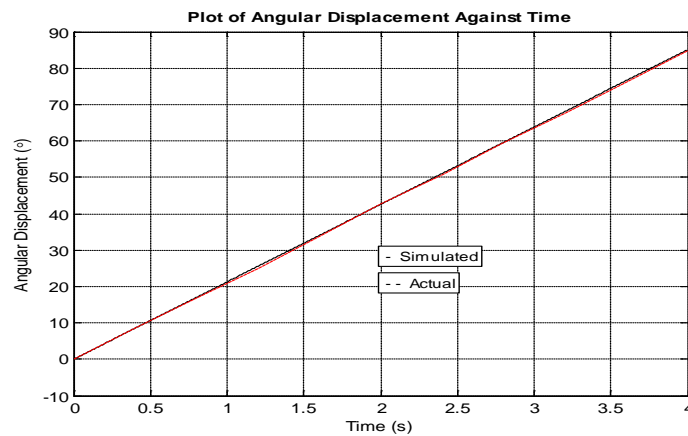
(a) Angular displacement for base



(b) Angular displacement for shoulder



(c) Angular displacement for elbow



(d) Angular displacement for wrist (pitch)

**Figure 4. Angular Displacements for each Simulated Joint**

## 5. Discussion

The simulated and actual angular displacement results are close in each case. However, the current model does not include the torque,  $T_D$ , which is required to produce the force to move the arm of the robot. The HSM torque,  $T_G$ , has to overcome this torque apart from the ones given in eq. (7). In addition, some estimated parameters were used in the model and the actual angular displacement of the robot in each case was manually measured. These could be some of the reasons for the variation between the two readings.

Better instrumentation, more accurate values of the estimated parameters used in the simulation, and determining a more complete model could be some of the ways to achieve more conforming results.

## 6. Conclusion

The mathematical model of a HSM has been used to understand the dynamics of the motions of the base, shoulder, elbow, and wrist (pitch) of the pick-and-place robot. The outputs of the simulated model are angular displacement and angular velocity but due to limitations in instrumentation, only the results for angular displacement were compared

against the actual angular displacement. While the model is not a complete one, it gives a good approximation of the angular displacement of each motion.

However, further work is needed to get a more accurate model of the physical system. Also, the angular velocity needs to be measured to determine parameters such as settling time and overshoot which can in turn be used to determine the damping of the system.

## Acknowledgements

This work was funded by the University Research Committee at the University of the South Pacific under research grant 6C066.

## References

- [1] S. N. Yu, S. J. Lim, C. S. Han, M. K. Kang and S. R. Kim, "Development of a robot simulator using a modified trajectory generation algorithm oriented towards the palletizing task", Proceedings of the Institution of Mechanical Engineers, Part C: Journal of Mechanical Engineering Science, vol. 222, no. 7, (2008) July, pp. 1253-1264.
- [2] H. M. Do, C. Park and J. H. Kyung, "Dual arm robot for packaging and assembling of IT products", 2012 IEEE International Conference on Automation Science and Engineering (CASE), (2012) August 20-24, pp. 1067-1070.
- [3] C. Park, K. Park and D. Kim, "Design of dual arm robot manipulator for precision assembly of mechanical parts", International Conference on Smart Manufacturing Application 2008 (ICSMA 2008), (2008) April 9-11, pp. 424-427.
- [4] B. Roy and H. H. Asada, "Design of a Reconfigurable Robot Arm for Assembly Operations inside an Aircraft Wing-Box", Proceedings of the 2005 IEEE International Conference on Robotics and Automation (ICRA 2005), (2005) April 18-22, pp. 590-595.
- [5] M. J. Bakari, K. M. Zeid and D. W. Seward, "Development of a multi-arm mobile robot for nuclear decommissioning tasks", International Journal of Advanced Robotic Systems, vol. 4, no. 4, (2007), pp. 387-406.
- [6] C. Lenz, S. Nair, M. Rickert, A. Knoll, W. Rosel, J. Gast, A. Bannat and F. Wallhoff, "Joint-action for humans and industrial robots for assembly tasks", The 17th IEEE International Symposium on Robot and Human Interactive Communication 2008 (RO-MAN 2008), (2008) August 1-3, pp. 130-135.
- [7] S. R. Cruz-Ramirez, Y. Ishizuka, Y. Mae, T. Takubo and T. Arai, "Dismantling interior facilities in buildings by human robot collaboration", IEEE International Conference on Robotics and Automation 2008 (ICRA 2008), (2008) May 19-23, pp. 2583-2590.
- [8] R. V. Sharan, "A vision-based pick-and-place robot", MSc Thesis, Department of Engineering, University of the South Pacific, Suva, Fiji, (2006) June.
- [9] R. V. Sharan and G. C. Onwubolu, "Development of a vision-based pick-and-place robot", Proceedings of the 3<sup>rd</sup> International Conference on Autonomous Robots and Agents (ICARA), Palmerston North, New Zealand, (2006) December 12-14, pp. 473-478.
- [10] A. Morar, "Stepper motor model for dynamic simulation", ACTA Electrotehnica, vol. 44, no. 2, (2003), pp. 117-122.
- [11] P. Chand, G. C. Onwubolu and S. Kumar, "Modeling and simulation of a PC-based computer numerically controlled drilling machine worktable", Proceedings of the Institution of Mechanical Engineers, Part B: Journal of Engineering Manufacture, vol. 218, no. 11, (2004) November, pp. 1625-1630.
- [12] G. C. Onwubolu, S. Aborhey, R. Singh, H. Reddy, M. Prasad, S. Kumar and S. Singh, "Development of a PC-based computer numerical control drilling machine", Proceedings of Institute of Mechanical Engineers, Part B: Journal of Engineering Manufacture, vol. 216, no. 11, (2002), pp. 1509-1515.
- [13] S. Kumar and G. C. Onwubolu, "A roaming vehicle for entity relocation", Proceedings of the Virtual International Conference on Intelligent Production Machines and Systems (Eds D.T. Pham, E. E. Eldukhri, and A. J. Soroka), (2005), pp. 135-139.
- [14] S. P. Lal and G. C. Onwubolu, "Three tiered web-based manufacturing system-Part 1: system development", Journal of Robotics and Computer-Integrated Manufacturing, vol. 23, no. 1, (2007), pp. 138-151.
- [15] R. V. Sharan and G. C. Onwubolu, "Client-server control architecture for a vision-based pick-and-place robot", Proceedings of the Institution of Mechanical Engineers, Part B: Journal of Engineering Manufacture, vol. 228, no. 8, (2012) August, pp. 1369-1378.
- [16] RS Data Sheet 425-6241: stepper motor drive boards, RS Components, Australia, (2002).
- [17] RS Data Sheet 314-2258: hybrid stepper motors, RS Components, Australia, (2002).